Electronic Supplementary Information (ESI)

U– to Z–shape isomerization in Pt_2Ag_2 framework containing pyridyl-NHC ligands

Shinnosuke Horiuchi,[a] Sangjoon Moon,[a] Eri Sakuda,[a] Akitaka Ito,[b] Yasuhiro Arikawa,[a] and Keisuke Umakoshi*[a]

[a]*Division of Chemistry and Materials Science, Graduate School of Engineering, Nagasaki University, Bunkyo-machi, Nagasaki 852-8521, Japan. E-mail: kumks@nagasaki-u.ac.jp*
[b]*Graduate School of Engineering/School of Environmental Science and Engineering, Kochi University of Technology, 185 Miyanokuchi, Tosayamada, Kami, Kochi 782-8502, Japan*

Experimental section

Materials. (Py-NHC)$PtCl_2$ was prepared according to a modified literature method.[1] All other commercially available reagents were used as purchased. Synthesis of the complexes was carried out under air unless otherwise noted.

Physical Measurement and Instrumentation. The 1D (^1H, ^{13}C) and 2D (^1H-^1H COSY, ^1H-^{13}C HSQC, ^1H-^{13}C HMBC) NMR spectra were obtained at 500 MHz Varian NMR System 500PS spectrometer. The VT-NMR (variable-temperature NMR) measurements were performed at 400 MHz with JEOL JNM-AL400. UV/Vis spectra were recorded on a Jasco V-560 spectrophotometer at 20°C. The corrected emission spectra were obtained by using a Hamamatsu PMA-12 multichannel photodetector (excitation wavelength = 355 nm). Emission quantum yields in the solid state were determined by using a Hamamatsu Photonic Absolute PL Quantum Yield Measurement System C9920-02 with an integrating sphere and a PMA-12 multichannel photodetetor (excitation wavelength = 300 nm). The emission lifetime measurements were conducted by using a Hamamatsu C11200 streak camera as a photodetector by exciting at 355 nm using a nanosecond Q-switched Nd:YAG laser (Continum® Minilite™, fwhm ≈ 10–12 ns, repetition rate = 10 Hz).

Preparation of Complexes.
[(Py-NHC)Pt(Me_2pzH)$_2$](PF_6)$_2$ ([**2**](PF_6)$_2$).

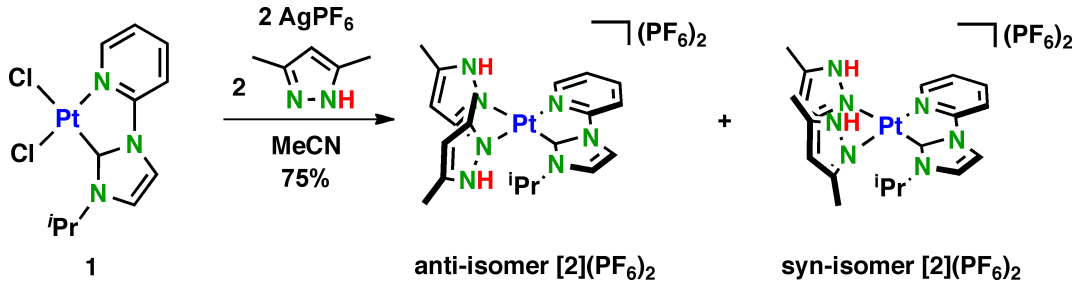

Scheme S1. Synthesis of [**2**](PF_6)$_2$.

A mixture of (Py-NHC)$PtCl_2$ (**1**) (257 mg, 0.57 mmol) and $AgPF_6$ (318 mg, 1.26 mmol) in acetonitrile (30 mL) was refluxed for 2 h. After the precipitate was removed by filtration, Me_2pzH (169 mg, 1.76 mmol) was added to the filtrate and stirred for 2 h at room temperature. The mixture was concentrated and diethyl ether was added to the solution. The resulted white precipitate was collected, washed with diethyl ether, and dried in vacuo, [(Py-NHC)Pt(Me_2pzH)$_2$](PF_6)$_2$ ([**2**](PF_6)$_2$) was isolated as a white solid. Yield 369 mg (75%). It was purified by recrystallization from an acetone/*n*-hexane solution. Anal. Calcd for $C_{21}H_{29}N_7PtP_2F_{12}$: C, 29.16; H, 3.38; N, 11.34. Found: C, 29.45; H, 2.90; N, 11.35. ^1H NMR

(500 MHz, CD_3CN, 298 K) of isomer mixture of [**2**]$(PF_6)_2$: δ = 11.8 (br, 2H, Me_2pzH), 11.6 (br, 1H, Me_2pzH), 11.4 (br, 1H, Me_2pzH), 8.37 (t, *J* = 9.0 Hz, 2H, Py), 7.99 (d, *J* = 2.5 Hz, 1H, NHC), 7.99 (d, *J* = 2.5 Hz, 1H, NHC), 7.92 (d, *J* = 8.5 Hz, 2H, Py), 7.62 (d, *J* = 6.0 Hz, 1H, Py), 7.49 (d, *J* = 2.5 Hz, 1H, NHC), 7.50–7.43 (m, 3H, Py), 6.26 (s, 1H, Me_2pzH), 6.23 (s, 2H, Me_2pzH), 6.22 (s, 1H, Me_2pzH), 2.98 (sept, *J* = 7.0 Hz, 1H, ^{i}Pr), 2.86 (sept, *J* = 7.0 Hz, 1H, ^{i}Pr), 2.40 (s, 6H, Me_2pzH), 2.39 (s, 3H, Me_2pzH), 2.36 (s, 3H, Me_2pzH), 2.34 (s, 3H, Me_2pzH), 2.33 (s, 3H, Me_2pzH), 2.30 (s, 3H, Me_2pzH), 2.29 (s, 3H, Me_2pzH), 1.32 (d, *J* = 7.0 Hz, 3H, ^{i}Pr), 1.31 (d, *J* = 7.0 Hz, 3H, ^{i}Pr), 1.28 (d, *J* = 7.0 Hz, 3H, ^{i}Pr), 1.27 ppm (d, *J* = 7.0 Hz, 3H, ^{i}Pr). ^{13}C NMR (125 MHz, CD_3CN, 298 K) of isomer mixture of [**2**]$(PF_6)_2$: δ = 154.0, 153.9, 153.0, 152.8, 152.6, 151.8, 150.3, 150.1, 147.0, 146.9, 146.8, 146.5, 145.7, 145.7, 144.6, 144.4, 125.4, 125.3, 121.0, 119.5, 119.4, 113.8, 113.8, 108.4 (Me_2pzH), 108.4 (Me_2pzH), 108.4 (Me_2pzH), 108.4 (Me_2pzH), 108.3 (Me_2pzH), 108.3 (Me_2pzH), 108.3 (Me_2pzH), 108.3 (Me_2pzH), 52.6 (^{i}Pr), 52.6 (^{i}Pr), 23.1 (^{i}Pr), 22.9 (^{i}Pr), 14.8 (Me_2pzH), 14.6 (Me_2pzH), 14.5 (Me_2pzH), 14.1 (Me_2pzH), 11.2 (Me_2pzH), 11.1 (Me_2pzH), 11.1 (Me_2pzH), 11.0 (Me_2pzH) ppm. FAB-MS for [**2**]$(PF_6)_2$: *m*/*z* = 573 [*M*–{H+2(PF_6)}]$^+$, 719 [M–(PF_6)]$^+$.

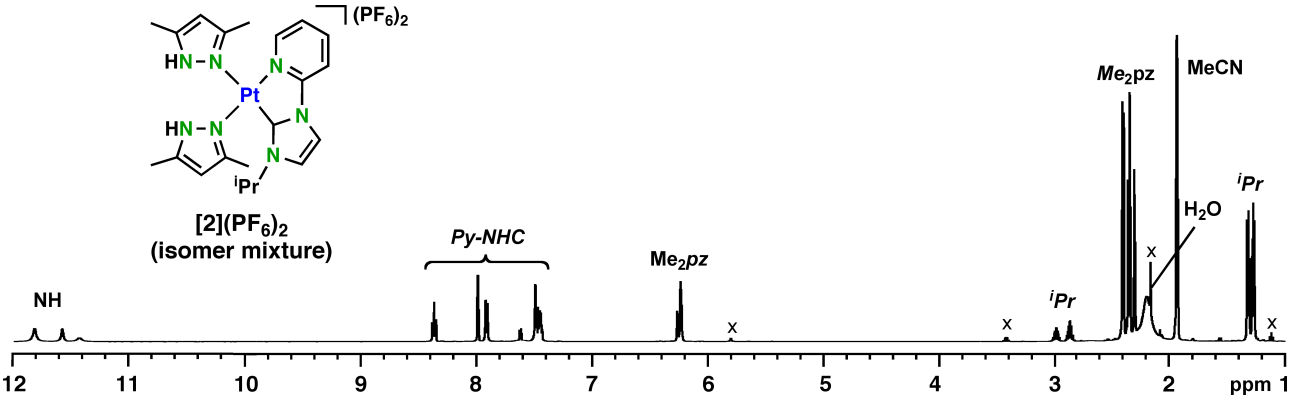

Figure S1. ^{1}H NMR spectrum (500 MHz, CD_3CN, 298 K) of [**2**]$(PF_6)_2$. Two sets of pyrazole–NH and ^{i}Pr signals indicate that Pt complex [**2**]$(PF_6)_2$ exists as a mixture of two geometrical isomers having syn- and anti-conformation at pyrazole moieties.

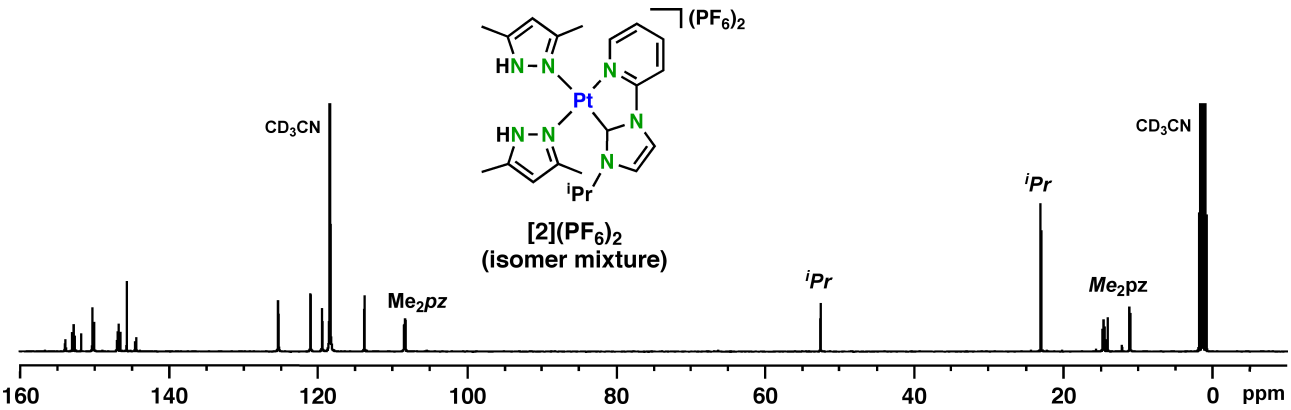

Figure S2. ^{13}C NMR spectrum (125 MHz, CD_3CN, 298 K) of [**2**]$(PF_6)_2$.

[(Py-NHC)Pt$_2$Ag$_2$(Me$_2$pz)$_4$](PF$_6$)$_2$ ([3](PF$_6$)$_2$).

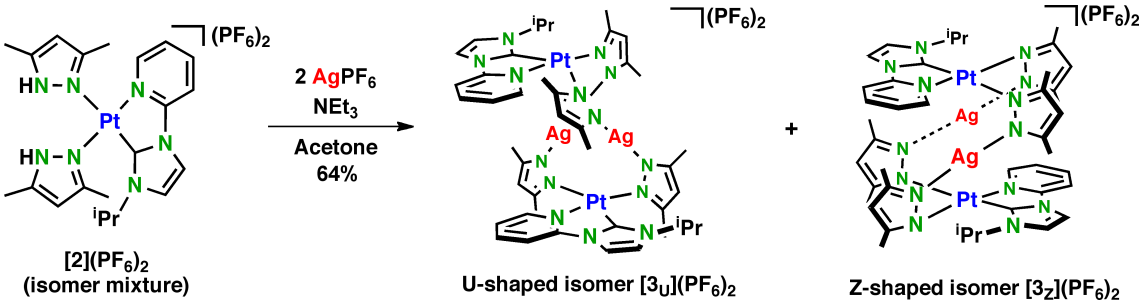

Scheme S2. Synthesis of [**3**](PF$_6$)$_2$.

To a solution of [**2**](PF$_6$)$_2$ (173 mg, 0.20 mmol) in acetone (10 mL) was added a solution of AgPF$_6$ (57 mg, 0.23 mmol) in acetone (10 mL) and triethylamine (60 μL, 0.43 mmol). The solution was stirred for 2 h at room temperature in the dark. After the solution was dried in vacuo, the residue was dissolved in dichloromethane. The organic layer was washed with water and dried over MgSO$_4$. After filtration, concentration in vacuo, and addition of *n*-hexane to the solution, isomer mixture of the Pt$_2$Ag$_2$ complex [**3**](PF$_6$)$_2$ was isolated as a white solid. Yield 106 mg (64%). U-shaped isomer [**3$_U$**](PF$_6$)$_2$ was selectively obtained by recrystallization from an acetone/*n*-hexane solution. Anal. Calcd for $C_{42}H_{54}Ag_2N_{14}Pt_2P_2F_{12}$: C, 30.58; H, 3.30; N, 11.89. Found: C, 30.79; H, 3.34; N, 12.01. ^{1}H NMR (500 MHz, $CDCl_3$, 298 K, TMS) of U-shaped isomer [**3$_U$**](PF$_6$)$_2$: δ = 8.17 (t, *J* = 8.0 Hz, 2H, Py), 7.97 (s, 2H, NHC), 7.86 (d, *J* = 8.0 Hz, 2H, Py), 7.28 (s, 2H, NHC), 7.16 (t, *J* = 8.0 Hz, 2H, Py), 6.87 (d, *J* = 6.0 Hz, 2H, Py), 6.09 (s, 2H, Me$_2$pzH), 6.02 (s, 2H, Me$_2$pzH), 2.93 (sept, *J* = 7.0 Hz, 2H, ^{i}Pr), 2.28 (s, 6H, Me$_2$pzH), 2.12 (s, 6H, Me$_2$pzH), 2.07 (s, 6H, Me$_2$pzH), 1.93 (s, 6H, Me$_2$pzH), 1.28 (d, *J* = 7.0 Hz, 6H, ^{i}Pr), 1.22 (d, *J* = 7.0 Hz, 6H, ^{i}Pr); Z-shaped isomer [**3$_Z$**](PF$_6$)$_2$: δ = 8.34 (t, *J* = 7.0 Hz, 2H, Py), 7.99 (d, *J* = 7.0 Hz, 2H, Py), 7.81 (s, 2H, NHC), 7.51 (t, *J* = 7.0 Hz, 2H, Py), 7.24 (d, *J* = 7.0 Hz, 2H, Py), 7.14 (s, 2H, NHC), 6.05 (s, 2H, Me$_2$pzH), 6.03 (s, 2H, Me$_2$pzH), 2.97 (sept, *J* = 7.0 Hz, 2H, ^{i}Pr), 2.23 (s, 6H, Me$_2$pzH), 2.20 (s, 6H, Me$_2$pzH), 2.14 (s, 6H, Me$_2$pzH), 1.99 (s, 6H, Me$_2$pzH), 1.19 (d, *J* = 7.0 Hz, 6H, ^{i}Pr), 0.89 (d, *J* = 7.0 Hz, 6H, ^{i}Pr) ^{13}C NMR (125 MHz, $CDCl_3$, 298 K, $CDCl_3$) of isomer mixture of the Pt$_2$Ag$_2$ complex [**3**](PF$_6$)$_2$: δ = 152.8, 152.6, 150.7, 150.7, 150.5, 150.5, 150.4, 150.4, 150.3, 150,3 149.0, 148.8, 148.8, 148.7, 148.7, 148.2, 148.2, 147.9, 147.7, 147.7, 144.7, 144.2, 124.6, 124.5, 119.7, 119.6, 118.9, 118.3, 113.2, 113.1, 106.3 (Me$_2$pzH), 105.8 (Me$_2$pzH), 105.3 (Me$_2$pzH), 105.1 (Me$_2$pzH), 51.1 (^{i}Pr), 50.9 (^{i}Pr), 23.8 (^{i}Pr), 22.9 (^{i}Pr), 22.5 (^{i}Pr), 22.3 (^{i}Pr), 14.7 (Me$_2$pzH), 14.6 (Me$_2$pzH), 14.5 (Me$_2$pzH), 14.2 (Me$_2$pzH), 14.1 (Me$_2$pzH), 14.1 (Me$_2$pzH), 13.8 (Me$_2$pzH), 13.3 (Me$_2$pzH) ppm. ESI-MS for [**3**](PF$_6$)$_2$: *m*/*z* 1504.7 $[M–(PF_6)]^+$.

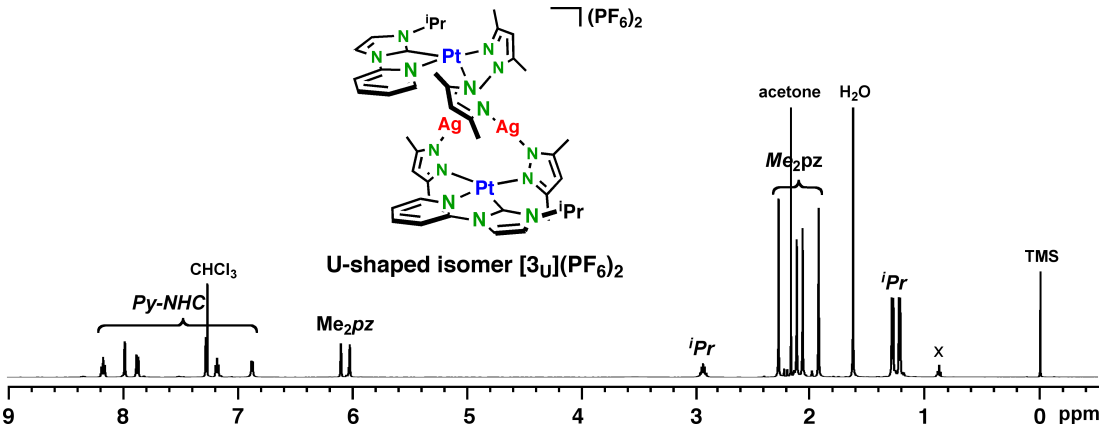

Figure S3. ^{1}H NMR spectrum (500 MHz, $CDCl_3$, 298 K) of U-shaped isomer $[\mathbf{3}_U](PF_6)_2$.

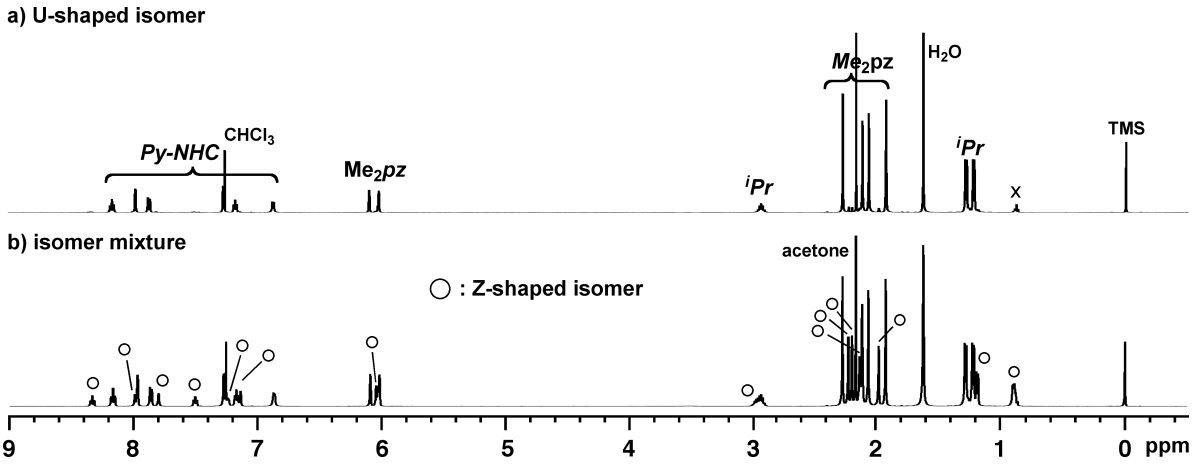

Figure S4. ^{1}H NMR spectra (500 MHz, $CDCl_3$, 298 K) of a) U-shaped isomer $[\mathbf{3}_U](PF_6)_2$ and b) $[\mathbf{3}](PF_6)_2$ consisting of two geometrical isomers (circles, Z-shaped isomer $[\mathbf{3}_Z](PF_6)_2$).

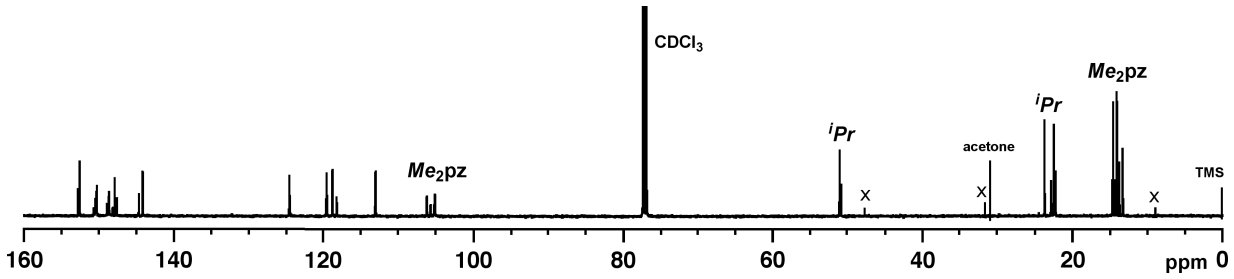

Figure S5. ^{13}C NMR spectrum (125 MHz, $CDCl_3$, 298 K) of $[\mathbf{3}](PF_6)_2$.

NMR studies

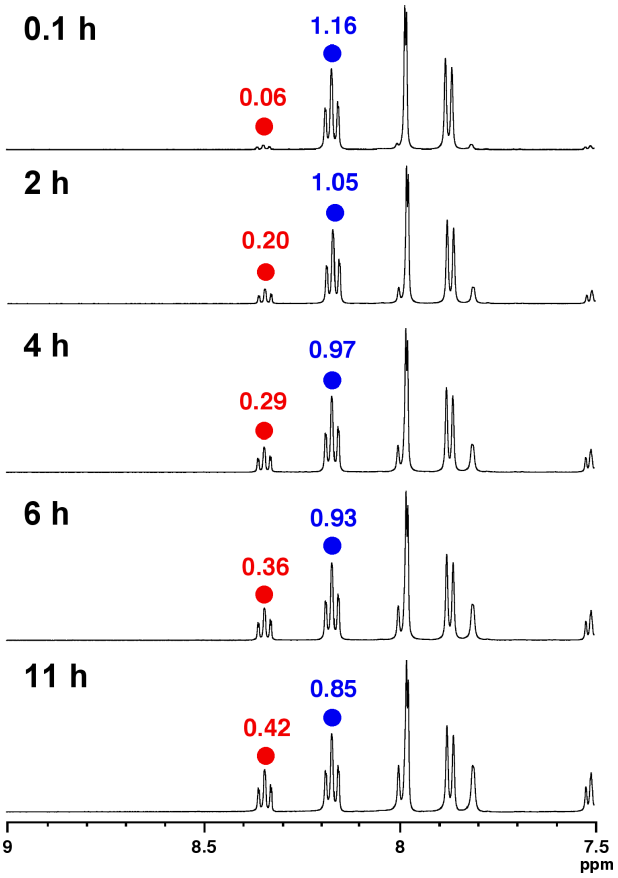

Figure S6. ^{1}H NMR spectral variations due to the isomerization of U-shaped isomer $[\mathbf{3}_{U}](PF_6)_2$ to Z-shaped isomer $[\mathbf{3}_{Z}](PF_6)_2$

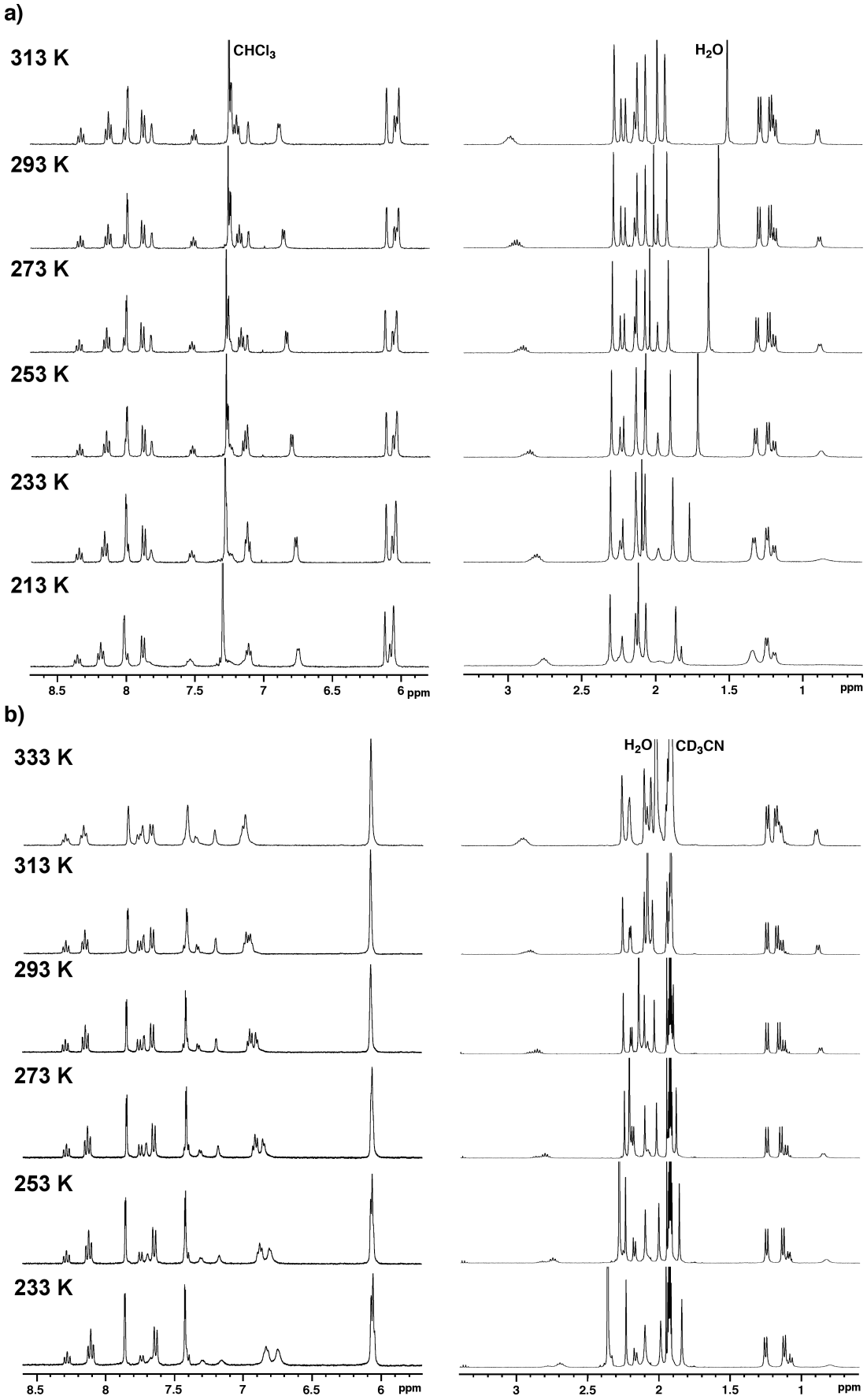

Figure S7. VT-NMR spectra (400 MHz) of [**3**]$(PF_6)_2$ in a) $CDCl_3$ and b) CD_3CN.

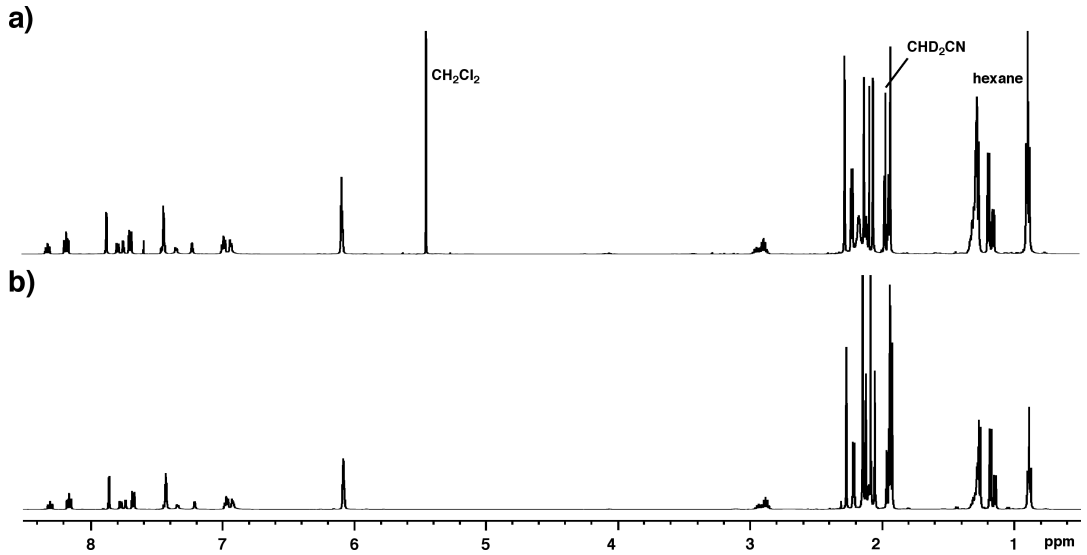

Figure S8. ^{1}H NMR spectra (500 MHz, CD_3CN, 300 K) of a) a crude reaction product of [**3**]$(PF_6)_2$ before recrystallization, and b) a solution within 5 minutes after single crystals of U-shaped isomer [$\mathbf{3}_U$]$(PF_6)_2$ were dissolved.

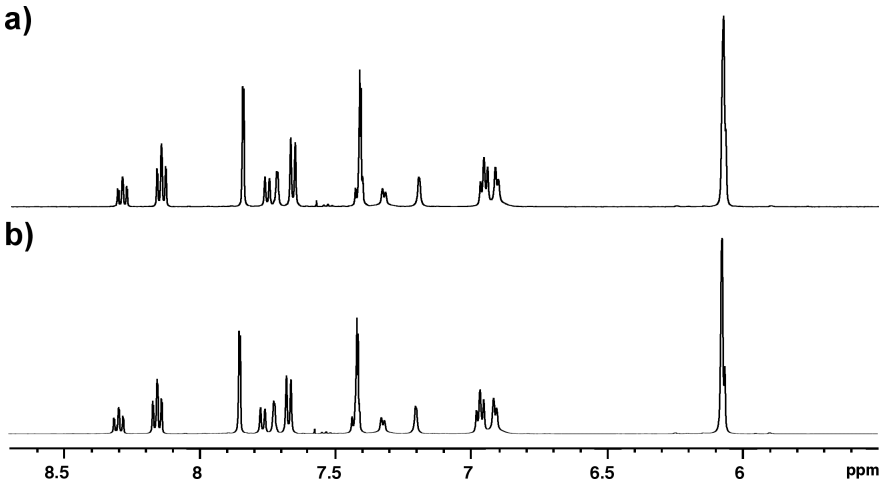

Figure S9. ^{1}H NMR spectra (500 MHz, CD_3CN, 300 K) of [**3**]$(PF_6)_2$ a) before and b) after an addition of $AgPF_6$ (1 eq.).

Photophysical data

All measurements were performed at room temperature. Emission decay curve was analysed by the equation ($I(t) = A_1\exp(-t/\tau_1) + A_2\exp(-t/\tau_2) + A_3\exp(-t/\tau_3)$) using the nonlinear least-squares method. The averaged emission lifetime (τ_{ave}) was estimated by the equation ($\tau_{ave} = (A_1\tau_1^2 + A_2\tau_2^2 + A_3\tau_3^2) / (A_1\tau_1 + A_2\tau_2 + A_3\tau_3)$).

Table S1. Photophysical data of [**2**]$(PF_6)_2$ and [**3**]$(PF_6)_2$ in the solid state at 298 K.

Complex	λ_{em} [nm]	Φ [%]	A_1	τ_1 [μs]	A_2	τ_2 [μs]	A_3	τ_3 [μs]	τ_{ave} [μs]
[**2**]$(PF_6)_2$	431	2	0.94	0.32	0.05	2.0	0.01	16.3	5.2
[**3**]$(PF_6)_2$	507	1	0.81	0.13	0.17	0.53	0.02	2.6	0.8

X-ray Structural Determinations.

Crystals suitable for X-ray structural analysis were obtained by recrystallization from acetone/*n*-hexane ([**2**](PF$_6$)$_2$), acetone/*n*-hexane ([**3**$_U$](PF$_6$)$_2$·3CH$_3$COCH$_3$) and CH$_3$CN/diethylether ([**3**$_U$][NHEt$_3$](PF$_6$)$_3$), respectively. The crystal structures were solved by direct method (SHELXS-97).[2] The positional and thermal parameters of non-H atoms were refined anisotropically by the full-matrix least-squares method except for disordering counter anions. All calculations were performed using the CrystalStructure crystallographic software package[3] except for refinement, which was performed using SHELXL-2014/7.[2]

Table S2. Crystallographic data for [(Py-NHC)Pt(Me$_2$pzH)$_2$](PF$_6$)$_2$ ([**2**](PF$_6$)$_2$), [(Py-NHC)$_2$Pt$_2$Ag$_2$(Me$_2$pz)$_4$](PF$_6$)$_2$·3(CH$_3$COCH$_3$) ([**3**$_U$](PF$_6$)$_2$·3CH$_3$COCH$_3$), [(Py-NHC)$_2$Pt$_2$Ag$_3$(Me$_2$pz)$_4$][NHEt$_3$](PF$_6$)$_3$ ([**3**$_U$][NHEt$_3$](PF$_6$)$_3$).

	[**2**](PF$_6$)$_2$	[**3**$_U$](PF$_6$)$_2$·3CH$_3$COCH$_3$	[**3**$_U$][NHEt$_3$](PF$_6$)$_3$
Empirical formula	$C_{21}H_{29}F_{12}N_7P_2Pt$	$C_{51}H_{72}Ag_2F_{12}N_{14}O_3P_2Pt_2$	$C_{48}H_{70}Ag_2F_{18}N_{15}P_3Pt_2$
Formula weight	864.53	1825.07	1897.99
Temperature (K)	93(1)	93(1)	93(1)
Wavelength (Å)	0.71075	0.71075	0.71075
Crystal system	monoclinic	monoclinic	orthorhombic
Space group	$P2_1/c$ (#14)	$P2_1/c$ (#14)	$Pna2_1$(#33)
Unit cell dimensions			
a (Å)	12.454(3)	13.5442(9)	13.402(2)
b (Å)	16.341(4)	16.5240(11)	29.139(5)
c (Å)	15.741(4)	29.6856(18)	16.427(3)
β (deg)	112.102(4)	90.7088(12)	90
V (Å^3)	2968.0(13)	6643.3(7)	6415.1(17)
Z	4	4	4
ρ_{calcd} (g/cm^3)	1.935	1.825	1.965
μ(Mo Kα) (mm^{-1})	4.918	4.892	5.104
F(000)	1680	3552	3680
Index ranges	-17<=h<=16	-16<=h<=17	-14<=h<=18
	-22<=k<=13	-21<=k<=21	-39<=k<=37
	-21<=l<=11	-30<=l<=38	-22<=l<=22
Reflections collected	16875	53334	57542
Independent reflections	7888 [R_{int} = 0.0266]	15082 [R_{int} = 0.0269]	17198 [R_{int} = 0.0739]
Data / restraints / parameters	7888 / 0 / 389	15082 / 0 / 767	17196 / 1 / 792
Goodness-of-fit on F^2	1.031	1.125	1.069
Final R index [I>2σ(I)][a]	R_1 = 0.0269	R_1 = 0.0257	R_1 = 0.0573
R indices (all data)[a,b]	R_1 = 0.0363, wR_2 = 0.0609	R_1 = 0.0283, wR_2 = 0.0773	R_1 = 0.0716, wR_2 = 0.1129
Largest diff. peak and hole (eÅ^{-3})	2.14 and –1.63	1.39 and –1.07	1.56 and –1.70
CCDC number	1588182	1588197	1588198

[a] $R_1 = \Sigma||F_o| - |F_c||/\Sigma|F_o|$. [b] $wR_2 = [\Sigma w(F_o^2 - F_c^2)^2]/\Sigma[w(F_o^2)^2]]^{1/2}$.

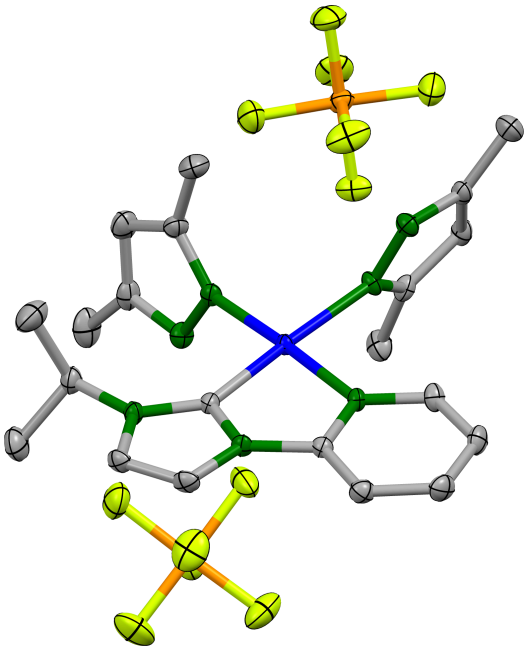

Figure S10. ORTEP drawing (50% probability ellipsoids) of [**2**]$(PF_6)_2$. Hydrogen atoms are omitted for clarity.

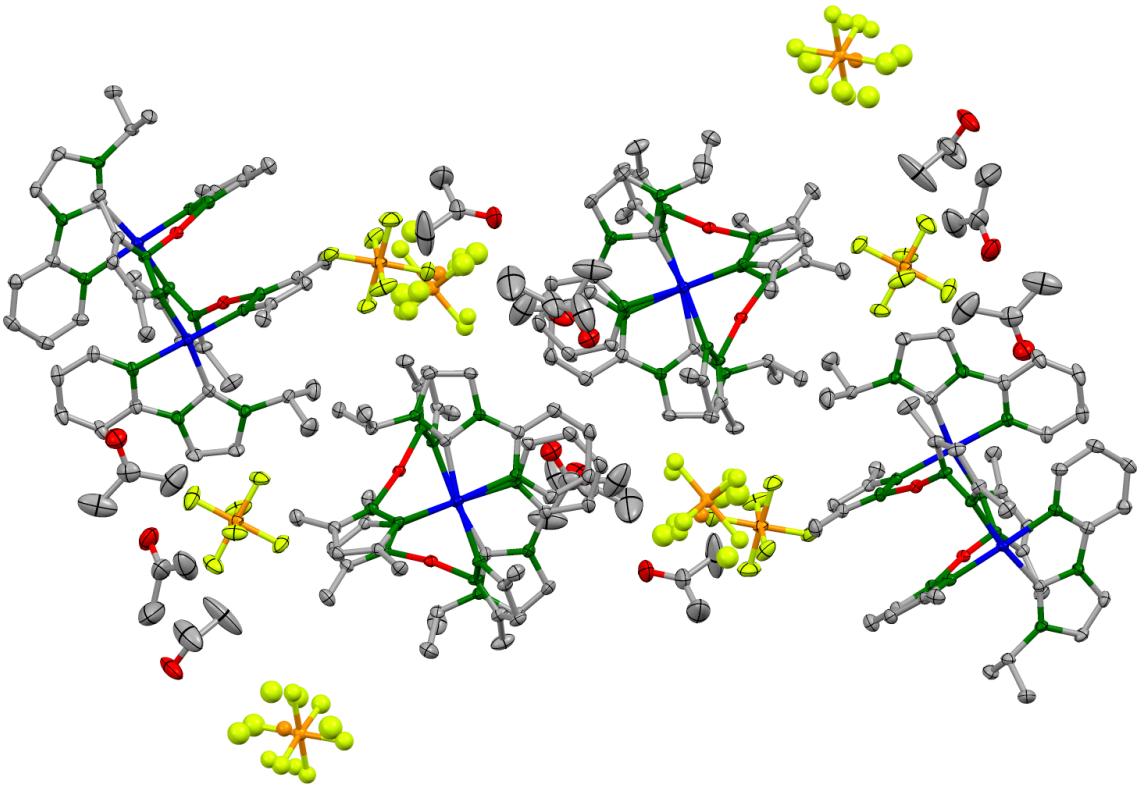

Figure S11. Crystal structure of [$\mathbf{3}_U$]$(PF_6)_2 \cdot 3CH_3COCH_3$. Hydrogen atoms are omitted for clarity.

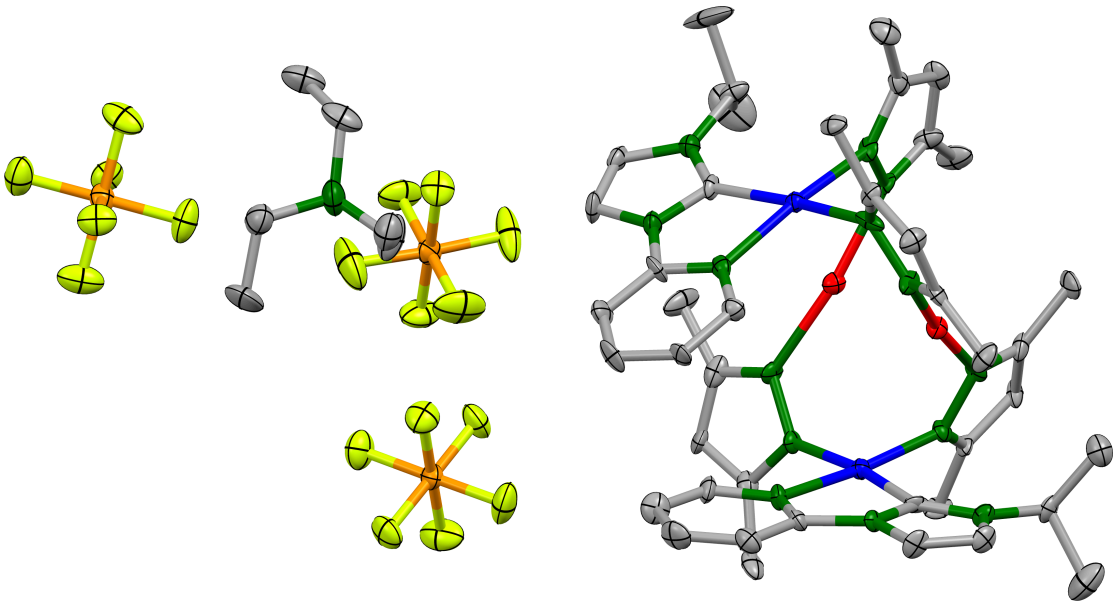

Figure S12. ORTEP drawing (50% probability ellipsoids) of $[\mathbf{3}_{U}][NHEt_3](PF_6)_3$. Hydrogen atoms are omitted for clarity. A single crystal of $[\mathbf{3}_{U}][NHEt_3](PF_6)_3$ was accidently obtained from the crude reaction mixture, containing a similar U-shaped Pt_2Ag_2 structure in the crystal.

Computational methods. Time-dependent density functional theory (TD-DFT) calculations were performed to estimate the energies and oscillator strengths of the 25 lowest-energy singlet and triplet absorption transitions by using the B3LYP DFT. The LanL2DZ and 6-31G(d,p) basis sets were used to treat the geometrical structures of the platinum/silver and all other atoms, respectively. For all of the calculations, crystallographic data were used as geometries in the crystalline phase. All calculations were carried out using the Gaussian 16W package.[4] Molecular orbitals with the isovalue of 0.03 were drawn by the Gauss View 5.[5]

Table S3. Calculated excited energies of $[(\text{Py-NHC})\text{Pt}(\text{Me}_2\text{pzH})_2]^{2+}$ ($[\mathbf{2}]^{2+}$).[a]

Excited State	Transition	Energy (Wavelength)	Oscillator Strength
S1	HOMO–2 → LUMO (15%) HOMO → LUMO (85%)	3.7637 eV (329.42 nm)	0.0090
S2	HOMO–2 → LUMO (30%) HOMO–1 → LUMO (70%)	3.9747 eV (311.94 nm)	0.0148
S3	HOMO–2 → LUMO (00%)	4.1890 eV (295.97 nm)	0.0089
S4	HOMO–6 → LUMO (36%) HOMO–5 → LUMO (64%)	4.4130 eV (280.95 nm)	0.0074
S5	HOMO–6 → LUMO (11%) HOMO–5 → LUMO (20%) HOMO–3 → LUMO (69%)	4.4557 eV (278.26 nm)	0.0029
S6		4.6519 eV (266.52 nm)	0.0075
S7		4.7125 eV (263.10 nm)	0.0042
S8		4.7426 eV (261.43 nm)	0.0800
S9		4.8221 eV (257.12 nm)	0.0009
S10		4.8405 eV (256.14 nm)	0.0640
S11		5.0280 eV (246.59 nm)	0.0816
S12		5.1135 eV (242.46 nm)	0.0040
S13		5.1848 eV (239.13 nm)	0.0860
S14		5.2234 eV (237.36 nm)	0.0085
S15		5.3731 eV (230.75 nm)	0.0154
S16		5.3889 eV (230.07 nm)	0.0019
S17		5.4252 eV (228.54 nm)	0.0023
S18		5.6013 eV (221.35 nm)	0.0558
S19		5.6472 eV (219.55 nm)	0.0162
S20		5.6586 eV (219.11 nm)	0.0843
S21		5.7000 eV (217.52 nm)	0.0849
S22		5.7874 eV (214.23 nm)	0.0126
S23		5.8227 eV (212.93 nm)	0.0806
S24		5.8491 eV (211.97 nm)	0.0115
S25		5.9323 eV (209.00 nm)	0.0018

[a] Transition details for S6–S25 are omitted.

Table S4. Molecular-Orbital Populations of $[(\text{Py-NHC})\text{Pt}(\text{Me}_2\text{pzH})_2]^{2+}$ ($[\mathbf{2}]^{2+}$).

Molecular Orbital	MO Population / %				
	Pt	Py-NHC		Me_2pz (trans to Py)	Me_2pz (trans to NHC)
		Py	NHC		
LUMO	9.88	67.36	18.86	2.42	1.48
HOMO	23.35	2.70	6.85	10.11	56.99
HOMO–1	22.84	4.94	30.53	38.71	2.98
HOMO–2	13.19	7.63	23.53	25.32	30.33
HOMO–3	2.71	2.00	4.02	9.65	81.62
HOMO–4	10.16	0.97	2.07	82.11	4.69
HOMO–5	73.87	11.38	12.28	1.28	1.19
HOMO–6	63.76	26.52	1.92	7.19	0.61

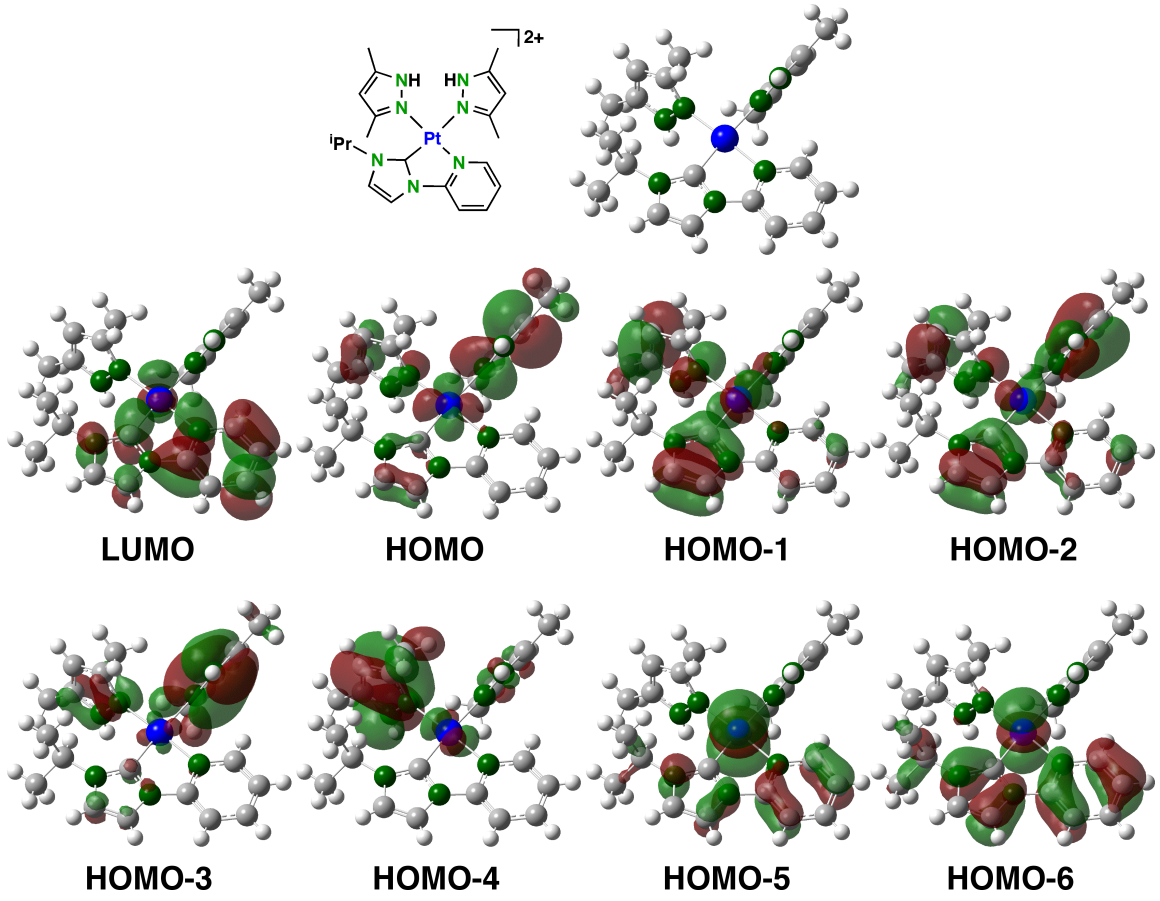

Figure S13. Molecular orbitals of the singlet state for $[(\text{Py-NHC})\text{Pt}(\text{Me}_2\text{pzH})_2]^{2+}$ ($[\mathbf{2}]^{2+}$).

Table S5. Calculated excited energies of $[(\text{Py-NHC})_2\text{Pt}_2\text{Ag}_2(\text{Me}_2\text{pz})_4]^{2+}$ ($[\mathbf{3}_\mathbf{U}]^{2+}$).[a]

Excited State	Transition	Energy (Wavelength)	Oscillator Strength
S1	HOMO–2 → LUMO (16%) HOMO–1 → LUMO (20%) HOMO → LUMO (64%)	2.7303 eV (454.11 nm)	0.0063
S2	HOMO–2 → LUMO+1 (14%) HOMO–1 → LUMO (31%) HOMO–1 → LUMO+1 (55%)	2.7560 eV (449.88 nm)	0.0052
S3	HOMO–1 → LUMO (62%) HOMO → LUMO+1 (38%)	2.9388 eV (421.88 nm)	0.0004
S4	HOMO–1→ LUMO+1 (44%) HOMO → LUMO (24%) HOMO → LUMO+1 (32%)	2.9497 eV (420.32 nm)	0.0022
S5	HOMO–2 → LUMO (57%) HOMO–1 → LUMO (22%) HOMO → LUMO+1 (21%)	2.9819 eV (415.80 nm)	0.0002
S6		2.9984 eV (413.50 nm)	0.0004
S7		3.0142 eV (411.33 nm)	0.0020
S8		3.0250 eV (409.87 nm)	0.0032
S9		3.0482 eV (406.75 nm)	0.0075
S10		3.0949 eV (400.61 nm)	0.0067
S11		3.1207 eV (397.30 nm)	0.0048
S12		3.1712 eV (390.97 nm)	0.0067
S13		3.2101 eV (386.23 nm)	0.0022
S14		3.2195 eV (385.10 nm)	0.0028
S15		3.2388 eV (382.81 nm)	0.0008
S16		3.2710 eV (379.04 nm)	0.0055
S17		3.3150 eV (374.01 nm)	0.0080
S18		3.3339 eV (371.89 nm)	0.0114
S19		3.4255 eV (361.94 nm)	0.0006
S20		3.4542 eV (358.93 nm)	0.0001
S21		3.4636 eV (357.96 nm)	0.0011
S22		3.4916 eV (355.09 nm)	0.0002
S23		3.6359 eV (341.00 nm)	0.0028
S24		3.6678 eV (338.03 nm)	0.0043
S25		3.7072 eV (334.44 nm)	0.0018

[a] Transition details for S6–S25 are omitted.

Table S6. Molecular-Orbital Populations of $[(\text{Py-NHC})_2\text{Pt}_2\text{Ag}_2(\text{Me}_2\text{pz})_4]^{2+}$ ($[\mathbf{3}_\text{U}]^{2+}$).

Molecular Orbital	MO Population / %					
	Pt	Ag	Py-NHC		Me_2pz (trans to Py)	Me_2pz (trans to NHC)
			Py	NHC		
LUMO+1	9.05	2.15	73.40	11.77	2.13	1.50
LUMO	8.34	1.18	73.71	14.11	1.77	0.89
HOMO	19.33	4.25	2.45	2.64	56.50	14.83
HOMO–1	17.43	5.10	2.37	2.30	53.13	19.67
HOMO–2	6.97	19.79	0.52	2.42	61.95	8.35

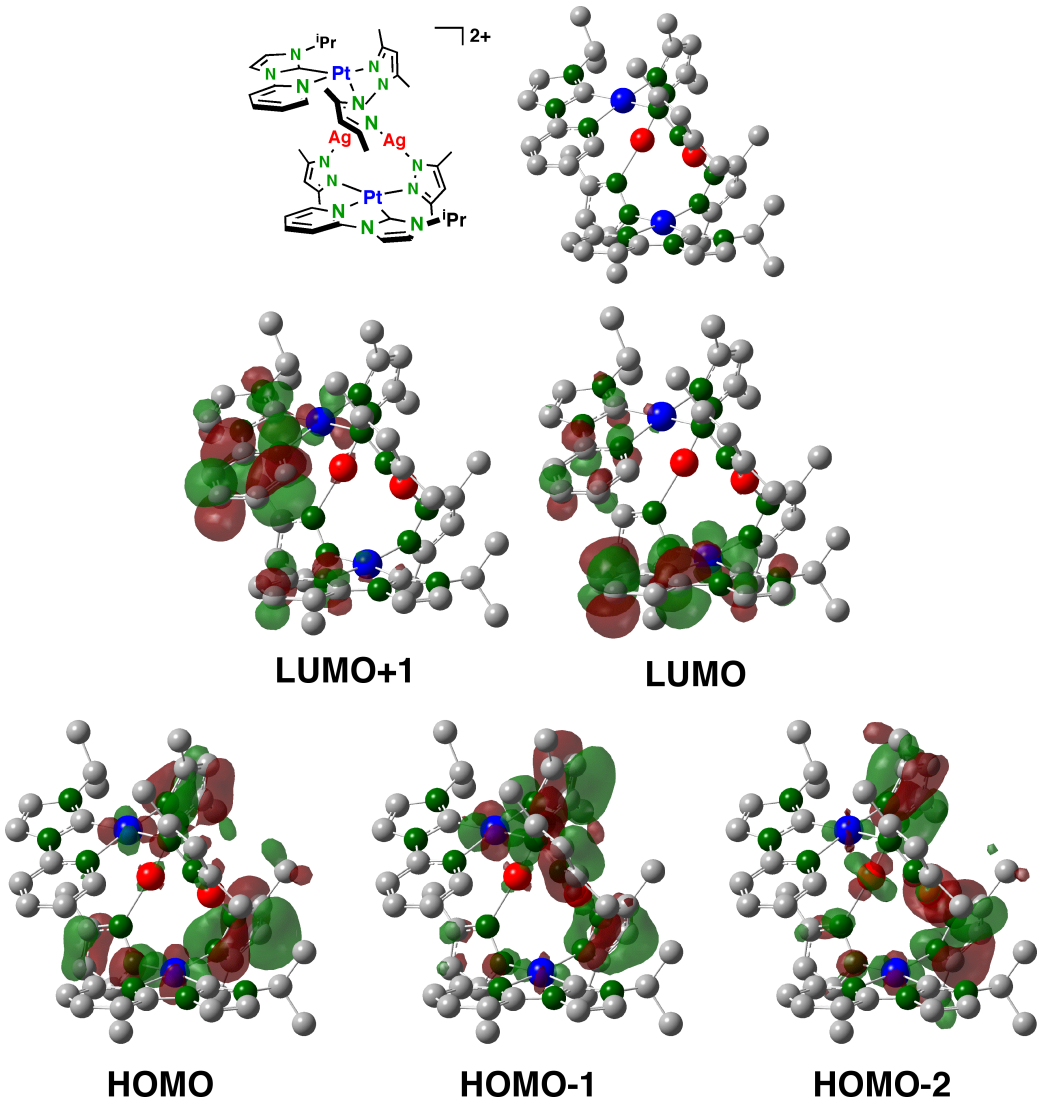

Figure S14. Molecular orbitals of the singlet state for $[(\text{Py-NHC})_2\text{Pt}_2\text{Ag}_2(\text{Me}_2\text{pz})_4]^{2+}$ ($[\mathbf{3}_\text{U}]^{2+}$). Hydrogen atoms are omitted for clarity.

References

1 P. Cao, J. Cabrera, R. Padilla, D. Serra, F. Rominger, M. Limbach, *Organometallics*, 2012, **31**, 921–929.

2 G. M. Sheldrick, *Acta Cryst*. 2008, **A64**, 112–122.

3 CrystalStructure 4.2: Crystal Structure Analysis Package, Rigaku Corporation, Tokyo, Japan, 2000–2017.

4 Gaussian 16, Revision A.03, M. J. Frisch, G. W. Trucks, H. B. Schlegel, G. E. Scuseria, M. A. Robb, J. R. Cheeseman, G. Scalmani, V. Barone, G. A. Petersson, H. Nakatsuji, X. Li, M. Caricato, A. V. Marenich, J. Bloino, B. G. Janesko, R. Gomperts, B. Mennucci, H. P. Hratchian, J. V. Ortiz, A. F. Izmaylov, J. L. Sonnenberg, D. Williams-Young, F. Ding, F. Lipparini, F. Egidi, J. Goings, B. Peng, A. Petrone, T. Henderson, D. Ranasinghe, V. G. Zakrzewski, J. Gao, N. Rega, G. Zheng, W. Liang, M. Hada, M. Ehara, K. Toyota, R. Fukuda, J. Hasegawa, M. Ishida, T. Nakajima, Y. Honda, O. Kitao, H. Nakai, T. Vreven, K. Throssell, J. A. Montgomery, Jr., J. E. Peralta, F. Ogliaro, M. J. Bearpark, J. J. Heyd, E. N. Brothers, K. N. Kudin, V. N. Staroverov, T. A. Keith, R. Kobayashi, J. Normand, K. Raghavachari, A. P. Rendell, J. C. Burant, S. S. Iyengar, J. Tomasi, M. Cossi, J. M. Millam, M. Klene, C. Adamo, R. Cammi, J. W. Ochterski, R. L. Martin, K. Morokuma, O. Farkas, J. B. Foresman, D. J. Fox, Gaussian, Inc., Wallingford CT, 2016.

5 GaussView, Version 5, R. Dennington, T. Keith J. Millam, Semichem Inc., Shawnee Mission, KS, 2009.